Published in final edited form as:
Oncogene. 2019 June 28; 38(31): 5971–5986. doi:10.1038/s41388-019-0853-z.

TBX2 interacts with heterochromatin protein 1 to recruit a novel repression complex to EGR1-targeted promoters to drive the proliferation of breast cancer cells

N. T. Crawford[#iD,1], **A.J. McIntyre**[#1], **A. McCormick**[1], **Z. C. D'Costa**[1], **N. E. Buckley**[iD,1], **P. B. Mullan**[1]

[1]Centre for Cancer Research and Cell Biology, Queen's University Belfast, Belfast BT9 7BL, UK

[#] These authors contributed equally to this work.

Abstract

Early Growth Response 1 (EGR1) is a stress response transcription factor with multiple tumour suppressor roles in breast tissue, whose expression is often lost in breast cancers. We have previously shown that the breast cancer oncogene TBX2 (T-BOX2) interacts with EGR1 to co-repress EGR1-target genes including the breast tumour suppressor NDRG1. Here, we show the mechanistic basis of this TBX2 repression complex. We show that siRNA knockdown of TBX2, EGR1, Heterochromatin Protein 1 (HP1) isoforms and the generic HP1-associated corepressor protein KAP1 all resulted in growth inhibition of TBX2-expressing breast cancer cells. We show that TBX2 interacts with HP1 through a conserved HP1-binding motif in its N-terminus, which in turn leads to the recruitment of KAP1 and other associated proteins. Mutation of the TBX2 HP1 binding domain abrogates the TBX2-HP1 interaction and loss of repression of target genes such as NDRG1. Chromatin-immunoprecipitation (ChIP) assays showed that TBX2 establishes a repressive chromatin mark, specifically H3K9me3, around the NDRG1 proximal promoter coincident with the recruitment of the DNA methyltransferase DNMT3B and histone methyltransferase (HMT) complex components (G9A, Enhancer of Zeste 2 (EZH2) and Suppressor of Zeste 12 (SUZ12)). Knockdown of G9A, EZH2 or SUZ12 resulted in upregulation of TBX2/EGR1 co-regulated targets accompanied by a dramatic inhibition of cell proliferation. We show that a generic inhibitor of HMT activity, DzNep, phenocopies expression of an inducible dominant negative TBX2. Knockdown of TBX2, KAP1 or HP1 inhibited NDRG1 promoter decoration specifically with the H3K9me3 repression mark. Correspondingly, treatment with a G9A inhibitor effectively reversed TBX2 repression of NDRG1 and synergistically downregulated cell proliferation following TBX2 functional inhibition. These data demonstrate that TBX2 promotes suppression of normal growth control mechanisms through recruitment of a large repression complex to EGR1-responsive promoters leading to the uncontrolled proliferation of breast cancer cells.

N. T. Crawford: 0000-0003-2258-4687

N. E. Buckley: 0000-0001-9326-8513

[✉]P. B. Mullan: p.mullan@qub.ac.uk.

Conflict of interest The authors declare that they have no conflict of interest.

Europe PMC Funders Author Manuscripts

Introduction

T-Box2 (TBX2) is a member of the T-box family of transcription factors, which play important roles in developmental gene regulation, especially in the embryonic development of mammary tissue [1]. TBX2 is located on chromosome 17q23, a region amplified in approximately 20% of primary breast tumours, most notably in high grade tumours and in BRCA1 and BRCA2 mutant breast cancers [2, 3]. TBX2 appears to be consistently overexpressed following amplification of the 17q23 region [4] although other candidates such as the DNA repair gene RAD51C have been implicated as oncogenes encoded in this region [5]. TBX2 is a transcriptional repressor and has been shown to facilitate senescence bypass in *Bmi*$^{-/-}$ mouse embryo fibroblasts when moderately overexpressed [6] and to act as a potent immortalising gene by downregulating *Cdkn2a* (*p19*^{ARF}, p14^{ARF} in humans) and p21^{WAF1} [7]. TBX2 is known to have a role in maintaining proliferation and suppressing cell senescence in melanoma cells [8] and in the promotion of anchorage-independent growth and bypass of apoptotic pathways in adrenocortical carcinomas [9]. In addition, TBX2 is frequently overexpressed in a number of other cancer types including breast, pancreatic and skin cancers [10]. It has been shown to promote epithelial-mesenchymal transition and invasion of both normal and malignant breast cells [11].

Our group have shown that TBX2 may also act as a transcriptional corepressor through its ability to interact with the transcription factor EGR1 [12]. This TBX2-EGR1 interaction may be important for its senescence-bypass function since EGR1 is an important regulator of senescence and induces key genes such as NDRG1, TP53, CDKN1A/p21^{WAF1}, TGFβ and PTEN [13]. More recently Tbx2 has been shown to interact with active hypophosphorylated retinoblastoma protein (RB1) and this interaction has also been shown to alter TBX2-target gene specificity [14]. Finally, it has been shown that the senescence phenotype induced by the PML tumour suppressor can only occur following specific downregulation of TBX2 [15].

The Heterochromatin Protein 1 (HP1) family consists of three isoforms (α, β and γ) which are all thought to be involved in constitutive (pericentric and telomeric) and facultative (developmentally regulated) heterochromatin. HP1β and HP1γ have also been found at euchromatic sites, where they are presumed to play a role in transcriptional repression [16]. HP1 recruitment to specific chromatin regions is known to be regulated through histone methylation marks. For example, the methylation of histone H3 on lysine 9 (H3K9me) is thought to be important for localising HP1 to distinct chromosome regions; and both trimethylated H3K9 (H3K9me3) and HP1 isoforms are thought to be crucial for establishing and maintaining heterochromatin regions [17]. The Kruppel-Associated Box-Associated Protein 1 (KAP1, also called TRIM28, TIF1β or KRIP-1) is a universal corepressor protein for the KRAB zinc finger protein (KRAB-zfp) superfamily of transcriptional repressors and is tethered to DNA through association with HP1 proteins. KAP1 then acts as a scaffold for various heterochromatin-inducing factors, such as further recruitment of HP1, histone methyltransferases (HMT), the nucleosome-remodelling and histone deacetylation (NuRD) complex, the nuclear receptor corepressor complex 1 (N-CoR1) and de novo DNA methyltransferases. The HMT complex EZH2/SUZ12/EED is known to decorate genomic

regions with the H3K27me3 chromatin mark but SUZ12 performs a dual role in this complex and may also facilitate H3K9me3 mediated silencing [18].

Here, we show the mechanistic basis of the TBX2-EGR1 repression complex and highlight the importance of this complex in maintaining the proliferation of TBX2-expressing breast cancers. We show that siRNA knockdown of TBX2, EGR1, HP1γ and KAP1 all result in growth inhibition in TBX2 expressing breast cancer cells. We show that TBX2 interacts with HP1γ and KAP1 through a conserved HP1-binding motif (PxVxL) in the TBX2 N-terminus and mutation of this motif abrogates the ability of TBX2 to interact with either protein or to repress target genes such as NDRG1. We show that TBX2 establishes a repressive (H3K9me3) chromatin mark around the NDRG1 proximal promoter through recruitment of histone methyltransferases, such as G9A and members of the Polycomb Repressor Complex 2, such as EZH2 and SUZ12. Finally we show through genetic inhibition of TBX2 and chemical inhibition of pan-histone methyltransferase (DzNeP) or G9A (BIX-01294) activity that we can effectively inhibit the proliferation of TBX2 expressing tumours, providing a novel therapeutic opportunity to target TBX2-expressing cancers.

Results

Knockdown of KAP1 and HP1 phenocopies knockdown of TBX2 in breast cancer cells

We have previously shown that TBX2 corepresses a number of genes including NDRG1 through its association with EGR1 [12]. Little is known about the mechanistic basis of TBX2 mediated repression or the likely corepressors or chromatin modifying proteins involved, although a C-terminal region of TBX2 has been shown to interact with histone deacetylase 1 (HDAC1) to target repression of the $p21^{WAF1}$ promoter [8]. We initially performed a small siRNA screen of known corepressor proteins and HDACs in MCF7 cells to identify likely repressor proteins whose expression was required to maintain MCF7 proliferation. One likely candidate which showed a consistent reduction of MCF7 cell proliferation following siRNA knockdown was the KRAB Domain–Associated Protein 1 (KAP1)/TRIM28 (Fig. 1a (i)). We also observed cell growth inhibition following knockdown of several HDACs (Fig. 1a (ii)). KAP1 serves as a universal, obligatory corepressor for over 220 members of the KRAB (Kruppel-Associated Box) domain zinc-finger protein superfamily of transcription factors [19]. It is known to interact with HP1 through its chromoshadow domain and is known to corepress target genes displaying promoter Histone 3 Lysine 9 trimethylation (H3K9me3), a well known repressive chromatin mark often observed in regions of heterochromatin [20]. We observed that KAP1 siRNA phenocopied both TBX2 and EGR1 knockdowns in terms of growth inhibition of MCF7 cells, producing significant growth inhibitory effects of at least 50% (Fig. 1b (i)-(iii)). HP1 can exist as three different isoforms HP1-α, HP1-β and HP1-γ which appear to have roles in facultative heterochromatin formation (-α, -β), pericentric constitutive heterochromatin (-β) and repression of euchromatin (-γ), respectively. They can also homodimerise and heterodimerise adding to the complexity of their function [21]. We were therefore interested in determining which isoforms preferentially interacted with TBX2 to facilitate repression. We performed specific siRNA knockdowns of all three isoforms in MCF7 cells (Fig. 1c (i)-(iii)). Knockdown of one isoform in particular, HP1-γ, resulted in a significant decrease in

MCF7 cell proliferation/survival, suggesting that it may be the key isoform responsible. To address whether dependency on KAP1 and HP1-γ for proliferation was cell line-specific, knockdowns of these two proteins were repeated in 17q23-amplified BT474 and TBX2-dependent T47D breast cancer models alongside positive controls TBX2 and EGR1 (Supplementary Fig. 1). As observed in MCF7, knockdown of KAP1 and HP1-γ led to a significant decrease in clonogenic survival of BT474 and T47D cells, implying this phenomenon was not simply a clonogenic artefact but consistent between TBX2-dependent breast tumours.

TBX2 interacts with KAP1 and HP1 through a HP1 interaction motif

We therefore wanted to investigate if TBX2 physically interacted with KAP1 or any of the HP1 isoforms and if these interactions were required to maintain MCF7 proliferation. We first performed pulldown experiments using FLAG-tagged TBX2 which showed an interaction with GFP-tagged versions of all three HP1 proteins (Fig. 2a (i)). Pulldown of FLAG-TBX2 also demonstrated interaction with endogenous KAP1 and HP1 proteins (Fig. 2a (ii)). This interaction was confirmed in reverse via pulldown of endogenous HP1-γ, where we observed co-immunoprecipitation with endogenous TBX2, in addition to the obligatory HP1-γ binding partner KAP1 (Fig. 2a (iii)). We used luciferase reporter assays of the NDRG1 proximal promoter (known to be potently co-repressed by TBX2/EGR1) which showed that KAP1 and HP1-γ knockdowns also resulted in increased expression of NDRG1 promoter activity (Fig. 2b (i)). Using ChIP assays we were able to show localisation of KAP1 and all three HP1 isoforms to the NDRG1 promoter, in a manner similar to previous demonstration of TBX2 and EGR1 localisation [12] (Fig. 2b (ii)). Furthermore, knockdown of KAP1 in multiple cell models resulted in significant increases in mRNA expression of NDRG1, p21, IGFBP3 and ERRFI1 (Fig. 2c (i)-(ii)), which were previously confirmed as TBX2 and/or EGR1-regulated target genes [7, 12, 22]. Together these data demonstrate that TBX2 resides in a complex with KAP1-HP1 proteins and that this complex is required for the repression of TBX2/EGR1 co-regulated target genes in breast cancer cells.

The ability of TBX2 to recruit KAP1/HP1 proteins is puzzling since TBX2 does not contain a KRAB domain, a feature which is normally a pre-requisite for KAP1 recruitment, making a direct TBX2-KAP1 interaction unlikely. We therefore wanted to determine the mode of the TBX2-KAP1-HP1 interaction. HP1 interacting proteins are known to contain a well conserved pentameric binding motif PxVxL [23]. Interestingly, we were able to detect a fully conserved motif in the N-terminus of TBX2 (PKVTL) in addition to another semi-conserved sequence (PLVVQ). We hypothesised that TBX2 first recruits HP1 proteins which in turn leads to the recruitment of a HP1-associated repression complex containing KAP1. We first performed site-directed mutagenesis (SDM) of TBX2 to generate single and double mutants and following exogenous expression of both mutants we observed by co-IP that both TBX2 mutants had lost ability to interact with endogenous HP1 and KAP1 relative to wild-type TBX2 (Fig. 3a (i), (ii), respectively). When densitometry was performed and quantified for the mutants (relative to FLAG as an expression control), it was clear that the mutant proteins interacted disproportionately lower (3-fold to 5-fold) than the WT, even taking into account their lower expression levels (Fig. 3a (i), (ii)). This suggested that the HP1-binding motif is crucial for the ability of TBX2 to recruit this repression complex.

Expression of the TBX2 mutants was accompanied by loss of repression of NDRG1 promoter luciferase activity also (Fig. 3b (i)). Since NDRG1 is known to be induced following DNA damage we repeated this experiment in the presence of 1 μM doxorubicin (24 h). We observed that whilst wild-type TBX2 was able to reduce promoter activity by at least 50%, a TBX2 HP1 binding site point mutant was largely devoid of functional repression (Fig. 3b (ii)). Whilst the point mutation was targeted within the T-box DNA binding domain this did not appear to have gross adverse effects on protein folding as the FLAG-tagged mutant was still localised to the nucleus (Fig. 3c) and both single and double mutants retained interactions with EGR1 by co-IP (Fig. 3d). To demonstrate the importance of the TBX2-HP1 interaction for KAP1 recruitment to the NDRG1 promoter we overexpressed FLAG TBX2 wild-type and a HP1 mutant in TBX2 non-expressing U2OS cells (Fig. 3e (i)), which resulted in the recruitment of KAP1 by wild-type TBX2 but a much reduced recruitment by a HP1 point mutant (FL-TBX2mut1), as shown by ChIP assays (Fig. 3e (ii)). Together these data suggest that TBX2, through interaction with HP1, is able to recruit a repression complex to EGR1 responsive promoters to enforce promoter shut-down.

TBX2 interacts with both H3K9 and H3K27 histone methyltransferases (HMTs)

The KAP1-HP1 interaction is synonymous with the H3K9me3 modification and as many as 6 HMTs can catalyse this modification in addition to the monomethylation and di-methylation of the same lysine by the G9A/GLP heterodimer [24]. Most of the HMTs responsible for H3K9me3 modification are implicated in constitutive and facultative heterochromatin. In addition, the H3K9me3 modification can be performed in euchromatin by the PRC2 complex, an enzyme complex more commonly associated with H3K27 trimethylation [25]. Indeed, one PRC2 member, SUZ12, possesses a dual role in both H3K9 and H3K27 methylation and can alter the affinity of the EZH2 methyltransferase activity from K27-specific to K9-specific methylation [25]. By ChIP assay we observed TBX2-dependent recruitment of the H3K9-specific HMT SETDB1 (Fig. 4a (i)) and enhanced H3K9 trimethylation coinciding with interaction of FLAG-TBX2 with SUZ12 and repressive histone marks (Fig. 4a (ii)). In addition, endogenous TBX2 was found to interact with EZH2, SUZ12 and DNMT3b (Fig. 4b). SiRNA knockdowns of members of the PRC2 complex (EZH2, SUZ12) and the H3K9 mono/dimethylase G9A all resulted in upregulation of NDRG1 mRNA in MCF7 (Fig. 4c (ii)) and T47D (Fig. 4d (ii)) cells accompanied by increases in mRNA of TBX2/EGR1-target genes p21 and ERRFI1, an effect which was most prominent following the depletion of G9A. Knockdowns of each of the three methyltransferases resulted in a significant reduction in cell number coincident with the enhanced expression of these tumour suppressor genes (Fig. 4c (iii), 4d (iii)). Loss of each of these HMTs also significantly impaired long-term survival as assessed by clonogenic assays (Fig. 4c (iv-v), d (iv-v)). However, not all H3K9 HMTs may be important for TBX2-mediated proliferation since knockdown of SUV39H1/H2, and SETDB1 resulted in enhanced, not reduced, proliferation of MCF7 cells (Supplementary Fig. 2). Taken together, we hypothesised that TBX2 was therefore present in a large repression complex containing specific HMTs and possibly HDACs with functional roles in the repression of EGR1-responsive genes.

KAP1/HP1 and HMTs are recruited to the NDRG1 promoter in a TBX2-dependent manner

To interrogate the dependence on TBX2 for recruitment of this complex to the NDRG1 promoter we generated a tetracycline inducible (Tet-OFF), FLAG-tagged TBX2 dominant negative construct (DN-TBX2) to abrogate the ability of full length TBX2 to recruit interacting partners. This DN-TBX2 consisted of the N-terminal half of human TBX2 containing the entire T-BOX domain (amino acids 1–361), based on a similar mouse construct previously generated by the Goding group [7]. As the ChIP assays in Fig. 5a (i) show, induction of DN-TBX2 resulted in reduced recruitment of KAP1 and HP1-γ to the NDRG1 promoter (showing a more pronounced decrease in HP1-γ recruitment). In addition, we observed reduced recruitment of the PRC2 proteins EZH2, SUZ12, the H3K9me3 chromatin mark and the DNA methyltransferase DNMT3b around this promoter (Fig. 5a (ii); RqPCR quantification of ChIP assays for several of these regulators is shown in Fig. 5b). Time course cell growth experiments using the DN-TBX2 model also showed an increase in NDRG1 expression following DN-TBX2 induction, an effect augmented following treatment with the generic HMT inhibitor Deazaneplanocin A (DzNep) (Fig. 5c, d; Supplementary Fig. 4). Finally, we could demonstrate the importance of HMT function for TBX2-mediated proliferation since treatment of these cells with DzNeP closely reflected the growth inhibition observed following DN-TBX2 induction (Fig. 5e). These data show that TBX2 is required for the recruitment of multiple chromatin regulators to target promoters and that histone methylation activity is important in maintenance of TBX2-mediated promoter repression and cell proliferation in TBX2 expressing cells.

A TBX2-KAP1-HP1 complex targets the NDRG1 promoter driving G9A-dependent H3K9 methylation and NDRG1 repression

To define which chromatin mark was most important for TBX2 repression we performed TBX2 knockdowns followed by ChIP assays which showed that H3K9me3 decoration of the NDRG1 promoter was completely lost whilst H3K27me3 localisation remained unchanged (Fig. 6a). The importance of KAP1 and HP1-γ in the TBX2 repression process is demonstrated by the fact that their corresponding knockdowns (Fig. 6b) also resulted in loss of H3K9me3 localisation on the NDRG1 promoter, with H3K27me3 localisation again remaining unchanged (Fig. 6d). Of note, knockdown of KAP1 and HP1-γ led to a near-complete reduction in TBX2 protein, which was inconsistent with TBX2 mRNA changes (Fig. 6b, c), suggesting these cofactors may also play a positive role in the maintenance of TBX2 protein stability. TBX2 knockdown also resulted in a reduction in protein expression of the H3K9 and H3K27 HMTs G9A and EZH2, in addition to reductions in proliferation-associated proteins such as c-MYC, PARP and CDK1 (Fig. 6e; Supplementary Fig. 4). Interestingly, G9A mRNA levels following TBX2 knockdown did not change significantly while EZH2, c-MYC and CDK1 depletion appeared to occur transcriptionally (Fig. 6g). While EZH2 inhibition displayed little effect on abrogation of TBX2 function (Supplementary Fig. 3), time course treatment with the G9A inhibitor BIX-01294 resulted in reduced TBX2 and EZH2 protein expression, marked recovery of NDRG1 expression and reductions in proliferation associated proteins in MCF7 cells (Fig. 6f; Supplementary Fig. 4). While G9A inhibition reduced TBX2, EZH2 and CDK1 expression at a protein level, increase in NDRG1 expression and loss of c-MYC appeared to occur at a transcriptional level synonymous with the effects of TBX2 siRNA (Fig. 6g). Treatment of a second cell

model (T47D) with BIX-01294 also resulted in loss of TBX2, EZH2 and CDK1 expression at a protein level accompanied by transcriptional upregulation of NDRG1 (Fig. 6h; Supplementary Fig. 4). Finally, cell count experiments showed that treatment with the G9A inhibitor BIX-01294 not only reduced cell proliferation but also showed a synergistic effect when combined with induction of DN-TBX2 (Fig. 6i), which was not observed in a parallel experiment performed using an EZH2 inhibitor (Supplementary Fig. 3). These data together mechanistically demonstrate that TBX2 repression specifically requires G9A activity (with accompanying increased H3K9 methylation) to achieve shutdown of target promoters such as NDRG1 and consequently maintenance of cell proliferation. A diagram of the mechanism of TBX2-dependent repression of promoters such as NDRG1 is shown in Fig. 7.

Discussion

TBX2 is a potent transcriptional repressor and is known to play important roles in senescence-bypass and proliferation, most notably in diseases such as breast cancer where its genetic locus is amplified [4]. Whilst TBX2 has been shown to interact with HDAC1, the mechanistic basis of how it represses target genes is still poorly understood [8]. We provided the first evidence that TBX2 interacts with the stress response transcription factor EGR1, switching EGR1 function to repression, rather than as a direct transcriptional regulator [12]. In this study, we provide further evidence that TBX2 is able to recruit a large repression complex through a novel association with HP1. Inhibiting this TBX2-HP1 interaction (*via* siRNA knockdowns or mutations) effectively inhibited recruitment of numerous chromatin regulators to EGR1 responsive promoters such as NDRG1, loss of H3K9me3 decoration, recovery of NDRG1 expression and inhibition of cell proliferation. NDRG1 was also re-expressed following knockdown of multiple complex members including corepressor HMTs. The generic HMT inhibitor DzNep can recapitulate the effects of TBX2 inhibition suggesting that a specific HMT-based therapy (for example, targeting G9A or EZH2) may be particularly effective for TBX2 overexpressing breast cancers.

The importance of aberrant TBX2 expression in poor prognosis cancers is now becoming increasingly evident. TBX2 was first linked to cancer through its ability to drive senescence bypass [6], shown to be preferentially amplified in BRCA1 and BRCA2 tumours [4] and to be co-amplified with other poor prognosis genes such as ERBB2 and MYC [26]. TBX2 may impact senescence at multiple levels such as the physical interference with PML function [15] or interaction with other transcriptional regulators such as EGR1, known to be important for senescence enforcement [27]. TBX2 targeting of EGR1 transcription may occur alongside two other reported mechanisms of TBX2 mediated carcinogenesis, namely, the direct repression of p14Arf through T-box binding and the reprogramming of cell-cycle control through direct interaction with Rb1 [5, 13]. In addition to its ability to inhibit senescence it is known to play a role in other aggressive traits such as increasing the epithelial-mesenchymal transition and invasion of normal and malignant breast epithelial cells [11]. It has also been implicated in the anchorage-independent survival of adrenocortical carcinoma cells [9] and G2 arrest bypass of Rb family deficient MEFs, resulting in their ability to establish tumours in mouse recipients in collaboration with mutant Ras [28]. TBX2, therefore, appears to amplify and collaborate with other oncogenic

events in the cell, including co-amplified oncogenes or the mutation of key tumour suppressor genes, to drive tumorigenesis.

The roles of epigenetic regulators contributing to pathological processes is an area of increasing interest in breast cancer biology. Difficult to treat subtypes such as triple negative have been linked to increased EZH2 activity [29] with increasing levels of EZH2 in highly metastatic breast cancers [30], correlating with increased tumour proliferation in situ [31]. The aggressive features of EZH2 expressing breast cancers such as basal-like breast cancers have been attributed to a role for EZH2 in driving breast 'stemness' including the expression of progenitor-associated, and dual basal-luminal lineage genes [32]. Similarly, G9A has been shown to interact with SNAIL to drive EMT through the repression of E-Cadherin [33]. Transcription factors such as RUNX2 can selectively target genes for direct activation or repression through recruitment of G9A in a locus-specific manner, independent of its HMT activity [34], suggesting that G9A-associated complex members may also be important for regulation of specific subsets of genes. HMT activity is also a well known pre-requisite for DNMT activity and it is known that important breast tumour suppressor genes such as maspin are kept switched off in breast cancer through a co-ordinated HMT-DNMT repression mechanism [35]. Consequently, treatment of some breast cancer cell lines with the DMNT inhibitor 5-aza-2'-deoxycytidine can result in a chain reaction of epigenetic events including global decreases in H3 K9 dimethylation and recovery of expression of genes such as maspin [35]. DNMT3B, in particular, has been reported to be aberrantly overexpressed in a subset of breast cancer cell lines, contributing to a 'hypermethylator phenotype' which coincided with the repression of a subset of genes commonly downregulated in primary basal-like breast cancers [36].

We believe this study highlights the ability of TBX2 to hijack the normal transcriptional machinery in order to repress growth control genes and promote tumorigenesis. Through its ability to interact with HP1, KAP1 and associated transcriptional repressors, TBX2 is able to force transcriptional shutdown upon EGR1-dependent genes, many of which are important tumour suppressor genes in their own right. Rather than being restricted to binding to target genes involved in embryogenesis with T-box sites in their regulatory regions, the aberrant TBX2 overexpression observed in primary breast cancers would now theoretically be able to target a larger number of EGR1-dependent genes (and possibly genes regulated by other, as yet unidentified TBX2-interacting transcriptional regulators). The demonstrated co-dependence on HP1/KAP1, G9A and PRC2 proteins suggests that this complex may be targetable by inhibitors against several HMTs, a fact demonstrated by the observed anti-proliferative phenotypes induced following knockdown of individual complex members. So whilst TBX2 itself represents a difficult therapeutic target, the identification of this functional multicomponent complex (containing several histone and DNA modifying enzymes) would suggest that there are alternative and more amenable opportunities for the treatment of TBX2-expressing, poor prognosis breast cancers.

Materials and methods

Cell culture

Cell lines were purchased authenticated from ATCC and tested for mycoplasma contamination prior to conducting experiments. The MCF7 and BT474 cells were maintained in Dulbecco's modified Eagle's medium; T47D and U2OS cells were maintained in RPMI. All were supplemented with 10% foetal calf serum, 1 mM sodium pyruvate, 50 mg/ml penicillin–streptomycin and 2 mM L-glutamine (Life Technologies, Inc., Paisley, UK). MCF7 dominant-negative TBX2 cells (MCF7-DN) were maintained in MCF7 media supplemented with G418 (500 μg/ml), puromycin (1 μg/ml) and tetracycline (1 μg/ml). To induce DN-TBX2, cells were cultured without addition of tetracycline. All were grown in 5% CO2 in a humidified incubator.

Clonogenic assays, growth curves and epigenetic inhibitor treatments

For clonogenic assays MCF7 cells were treated with siRNA as described below and after 48 h cells were seeded at 4000 cells/cm^2 in 6-well dishes and grown for 7 days. Cells were then fixed and stained with crystal violet and quantified as described previously [37]. Cell counts and DzNep dose response treatments were performed on Tet-inducible DN-TBX2 MCF7 cells. Cells were seeded at 10,000 cells/cm^2 in 24-well dishes and left to adhere overnight before being washed three times with phosphate buffered saline, followed by medium containing (+Tet) or without (–Tet) 1 μg/ml tetracycline and with (DzNep) or without (blank) 5 μM Deazaneplanocin A. Triplicate wells were then taken at 24 h intervals and counted using a coulter counter. For time course experiments with EZH2 (UNC1999) and G9A (BIX-01294) inhibitors, parental MCF7 cells were seeded in 100 mm culture dishes overnight prior to treatment with predetermined doses of agents and samples harvested at 24 h intervals. For combination experiments with EZH2 (UNC1999) and G9A (BIX-01294) inhibitors, Tet-inducible DN-TBX2 MCF7 cells were seeded in 100 mm culture dishes overnight before being washed three times with phosphate buffered saline, followed by growth in medium containing (+Tet) or without (–Tet) 1 μg/ml tetracycline for 2 days. After this time approximate IC50 doses of inhibitor or vehicle (DMSO) were added to medium and cells incubated for a further 3 days prior to counting as before.

RNA preparation and cDNA synthesis

RNA was extracted from cells using RNA STAT-60 reagent (Tel-Test Inc, Friendswood, TX, USA) according to manufacturer's instructions. RNA was then reverse transcribed using the Transcriptor First Stand cDNA synthesis kit (Roche, Burgess Hill, UK) according to manufacturer's instructions.

Real-time quantitative PCR

Relative quantitative PCR was performed on a 96-well plate (MJ Research, Waltham, MA, USA) on the LightCycler 96 System (Roche Life Science), and analysed using Roche Lightcycler 96 software. Gene expression was determined relative to the expression of SDHA (Succinate Dehydrogenase Complex Flavoprotein Subunit A). Primer sequences are shown in Supplementary Material.

Europe PMC Funders Author Manuscripts

Western blot analysis and antibodies

Protein lysates were extracted as described [38]. The antibodies: TBX2 (07–318); HP1β (MAB2448), and PARP1 (Ab-2, #AM30-100UG) were obtained from Millipore (Billerica, MA, USA); EGR1 (Cell Signalling, Boston, MA, USA) (#4154) and Santa Cruz Biotechnology (Santa Cruz, CA, USA) (sc110X); C-MYC (sc-764) from Santa Cruz, CA, USA; sheep polyclonal antibody for NDRG1 (Dr James Murray, QUB); KAP1 (Bethyl Laboratories, Montgomery, TX, USA) (BL553); HP1α (#2616), HP1γ (#2619), EZH2 (AC22, #31475) all from Cell Signalling (Boston, MA, USA); Histone H3K9me3 (ab8898), Histone H3K27me3 (ab6002), G9A (ab40542), SUZ12 (ab12073), DNMT3B (ab2851) all from Abcam (Cambridge, UK); mouse polyclonal antibody for FLAG M2 Sigma (Gillingham, Dorset, UK) (F1804); CDK1 (610038) from BD Transduction Laboratories (NJ, USA). GAPDH antibody (#4699–9555) (Biogenesis, Poole, UK) and Vinculin antibody (#13901) (Cell Signalling, Boston, MA, USA) were used to show equal loading of protein. Densitometric values below each lane represent protein expression levels normalised to loading control.

Short interfering RNA experiments

Cells were transfected using Lipofectamine RNAiMAX transfection reagent (ThermoFisher Scientific, UK) according to manufacturer's instructions. Protein or RNA was collected from cells 72 h following treatment with 100 nM siRNA. SiRNA primer sequences are listed in Supplementary Material.

Luciferase assays

MCF7 and U2OS cells were seeded into six-well plates at a density of 300,000 cells/well, transfected with control (pGL3-basic empty vector) or containing the proximal promoter of NDRG1 cloned upstream of firefly luciferase and co-transfected with beta-galactosidase expression constructs. The collection of samples and assay of luciferase activities are as previously described [38].

Site-directed mutagenesis

Site-directed mutagenesis was carried out using Hot-Start KOD Polymerase (Novagen, Merck Chemicals Ltd., Nottingham, UK) according to the manufacturer's instructions. The putative HP1 binding site in the TBX2 sequence (forward Primer Mut1, 5'-ggtggaggacgaccccgaggtgacgctggagg-3' and Mut2 5'-gaggacgaccccgcggcgacgctggaggccaag-3' with bold and underlined bases changed) was mutated using a FLAG-tagged wild-type TBX2 construct as template. The mutant construct sequenced to confirm base changes before being used in the co-IP, luciferase and ChIP assays as described.

Co-immunoprecipitations

MCF7 cells were transfected for 24 h with empty vector and FLAG-TBX2 pcDNA3.1. Whole-cell lysates were prepared with ELB (0.5 mM DTT, 5 mM EDTA pH 8.0, 50 mM HEPES pH 7.5, 0.1% IGEPAL, 250 mM NaCl). For FLAGTBX2 IP, 50 ml of sheep anti-mouse IgG Dynabeads (Invitrogen) were conjugated with 3 μg of FLAG (M2) mouse

monoclonal antibody (Sigma) and 3 μg of negative control mouse IgG1 (Dako), and washed and precleared with sheep anti-mouse IgG Dynabeads (Invitrogen) before adding to the antibody-conjugated beads and rotated for 4 h (4 °C). Beads were washed three times with ELB, resuspended in 20 ml of 10× protein sample buffer and boiled (95 °C for 10 min). Protein samples were then analysed by western blot analysis.

Chromatin immunoprecipitations

This assay was carried out using the U2OS, parental MCF7 and Tet-inducible DN-TBX2 MCF7 cell lines. This method has been described in detail elsewhere [37]. Promoter primers were designed for the NDRG1 proximal promoter region, encompassing EGR1 binding site as detailed in ref. [12]. Finally, PCR products were run on a 1.8% TBE agarose gel, and viewed (Syngene ChemiGenius, Cambridge, UK). The amount of NDRG1 promoter-specific product present in each ChIP was also quantified using relative quantitative PCR.

Statistics

Statistically analysed experiments were performed with at least three biological replicates unless otherwise stated. Statistical analyses were performed by two-tailed Student's *t*-test. Values with $P < 0.05$ or smaller are considered as statistically significant.

Supplementary Material

Refer to Web version on PubMed Central for supplementary material.

Acknowledgements

Special thanks to Dr James Murray (Trinity College Dublin) for the kind gift of sheep anti-human NDRG1 antibody and Professor Max Costa (University of New York) for NDRG1 promoter luciferase constructs. This work was supported by grants from the Breast Cancer Campaign and Breast Cancer Now (NEC, AMCI, AMCC, ZCD'C, NEB, PBM).

References

1. Chapman DL, Garvey N, Hancock S, Alexiou M, Agulnik SI, Gibson-Brown JJ, et al. Expression of the T-box family genes, Tbx1-Tbx5, during early mouse development. Dev Dyn. 1996; 206:379–90. [PubMed: 8853987]
2. Roylance R, Gorman P, Harris W, Liebmann R, Barnes D, Hanby A, et al. Comparative genomic hybridization of breast tumors stratified by histological grade reveals new insights into the biological progression of breast cancer. Cancer Res. 1999; 59:1433–6. [PubMed: 10197608]
3. Tirkkonen M, Johannsson O, Agnarsson BA, Olsson H, Ingvarsson S, Karhu R, et al. Distinct somatic genetic changes associated with tumor progression in carriers of BRCA1 and BRCA2 germ-line mutations. Cancer Res. 1997; 57:1222–7. [PubMed: 9102202]
4. Sinclair CS, Adem C, Naderi A, Soderberg CL, Johnson M, Wu K, et al. TBX2 is preferentially amplified in BRCA1- and BRCA2-related breast tumors. Cancer Res. 2002; 62:3587–91. [PubMed: 12097257]
5. Barlund M, Monni O, Kononen J, Cornelison R, Torhorst J, Sauter G, et al. Multiple genes at 17q23 undergo amplification and overexpression in breast cancer. Cancer Res. 2000; 60:5340–4. [PubMed: 11034067]
6. Jacobs JJL, Keblusek P, Robanus-Maandag E, Kristel P, Lingbeek M, Nederlof PM, et al. Senescence bypass screen identifies TBX2, which represses Cdkn2a (p19(ARF)) and is amplified in a subset of human breast cancers. Nat Genet. 2000; 26:291–9. [PubMed: 11062467]

7. Prince S, Carreira S, Vance KW, Abrahams A, Goding CR. Tbx2 directly represses the expression of the p21WAF1 cyclin-dependent kinase inhibitor. Cancer Res. 2004; 64:1669–74. [PubMed: 14996726]
8. Vance KW, Carreira S, Brosch G, Goding CM. Tbx2 is over-expressed and plays an important role in maintaining proliferation and suppression of senescence in melanomas. Cancer Res. 2005; 65:2260–8. [PubMed: 15781639]
9. Ismail A, Bateman A. Expression of TBX2 promotes anchorage-independent growth and survival in the p53-negative SW13 adrenocortical carcinoma. Cancer Lett. 2009; 278:230–40. [PubMed: 19216023]
10. Abrahams A, Parker MI, Prince S. The T-box transcription factor Tbx2: Its role in development and possible implication in cancer. IUBMB Life. 2010; 62:92–102. [PubMed: 19960541]
11. Wang B, Lindley LE, Fernandez-Vega V, Rieger ME, Sims AH, Briegel KJ. The T box transcription factor TBX2 promotes epithelial-mesenchymal transition and invasion of normal and malignant breast epithelial cells. PLoS ONE. 2012; 7doi: 10.1371/journal.pone.0041355
12. Redmond KL, Crawford NT, Farmer H, D'Costa ZC, O'Brien GJ, Buckley NE, et al. T-box 2 represses NDRG1 through an EGR1-dependent mechanism to drive the proliferation of breast cancer cells. Oncogene. 2010; 29:3252–62. [PubMed: 20348948]
13. De Belle I, Huang RP, Fan Y, Liu C, Mercola D, Adamson ED. P53 and Egr-1 additively suppress transformed growth in HT1080 cells but Egr-1 counteracts p53-dependent apoptosis. Oncogene. 1999; 18:3633–42. [PubMed: 10380885]
14. Vance KW, Shaw HM, Rodriguez M, Ott S, Goding CR. The retinoblastoma protein modulates Tbx2 functional specificity. Mol Biol Cell. 2010; 21:2770–9. [PubMed: 20534814]
15. Martin N, Benhamed M, Nacerddine K, Demarque MD, Van Lohuizen M, Dejean A, et al. Physical and functional interaction between PML and TBX2 in the establishment of cellular senescence. EMBO J. 2012; 31:95–109. [PubMed: 22002537]
16. Li Y, Kirschmann DA, Wallrath LL. Does heterochromatin protein 1 always follow code? Proc Natl Acad Sci. 2002; 99:16462–9. [PubMed: 12151603]
17. Sims RJ, Nishioka K, Reinberg D. Histone lysine methylation: a signature for chromatin function. Trends Genet. 2003; 19:629–39. [PubMed: 14585615]
18. Frietze S, O'Geen H, Blahnik KR, Jin VX, Farnham PJ. ZNF274 recruits the histone methyltransferase SETDB1 to the 39 ends of ZNF genes. PLoS ONE. 2010; 5doi: 10.1371/journal.pone.0015082
19. Friedman JR, Fredericks WJ, Jensen DE, Speicher DW, Huang XP, Neilson EG, et al. KAP-1, a novel corepressor for the highly conserved KRAB repression domain. Genes Dev. 1996; 10:2067–78. [PubMed: 8769649]
20. Bannister AJ, Zegerman P, Partridge JF, Miska EA, Thomas JO, Allshire RC, et al. Selective recognition of methylated lysine 9 on histone H3 by the HP1 chromo domain. Nature. 2001; 410:120–4. [PubMed: 11242054]
21. Kwon SH, Florens L, Swanson SK, Washburn MP, Abmayr SM, Workman JL. Heterochromatin protein 1 (HP1) connects the FACT histone chaperone complex to the phosphorylated CTD of RNA polymerase II. Genes Dev. 2010; 24:2133–45. [PubMed: 20889714]
22. Della Ragione F, Cucciolla V, Criniti V, Indaco S, Borriello A, Zappia V. p21Cip1 gene expression is modulated by Egr1. A novel regulatory mechanism involved in the resveratrol anti-proliferative effect. J Biol Chem. 2003; doi: 10.1074/jbc.M300771200
23. Cowieson NP, Partridge JF, Allshire RC, McLaughlin PJ. Dimerisation of a chromo shadow domain and distinctions from the chromodomain as revealed by structural analysis. Curr Biol. 2000; 10:517–25. [PubMed: 10801440]
24. Wu H, Min J, Lunin VV, Antoshenko T, Dombrovski L, Zeng H, et al. Structural biology of human H3K9 methyltransferases. PLoS ONE. 2010; 5doi: 10.1371/journal.pone.0008570
25. De La Cruz CC, Kirmizis A, Simon MD, Isono KI, Koseki H, Panning B. The polycomb group protein SUZ12 regulates histone H3 lysine 9 methylation and HP1α distribution. Chromosom Res. 2007; 15:299–314.

26. Adem C, Soderberg CL, Hafner K, Reynolds C, Slezak JM, Sinclair CS, et al. ERBB2, TBX2, RPS6KB1, and MYC alterations in breast tissues of BRCA1 and BRCA2 mutation carriers. Genes Chromosom Cancer. 2004; 41:1–11. [PubMed: 15236312]
27. Krones-Herzig A, Adamson E, Mercola D. Early growth response 1 protein, an upstream gatekeeper of the p53 tumor suppressor, controls replicative senescence. Proc Natl Acad Sci. 2003; 100:3233–8. [PubMed: 12629205]
28. Vormer TL, Foijer F, Wielders CLC, te Riele H. Anchorage-independent growth of pocket protein-deficient murine fibroblasts requires bypass of G2 arrest and can be accomplished by expression of TBX2. Mol Cell Biol. 2008; 28:7263–73. [PubMed: 18936168]
29. Hartman ZC, Poage GM, Den Hollander P, Tsimelzon A, Hill J, Panupinthu N, et al. Growth of triple-negative breast cancer cells relies upon coordinate autocrine expression of the proinflammatory cytokines IL-6 and IL-8. Cancer Res. 2013; 73:3470–80. [PubMed: 23633491]
30. Moore HM, Gonzalez ME, Toy KA, Cimino-Mathews A, Argani P, Kleer CG. EZH2 inhibition decreases p38 signaling and suppresses breast cancer motility and metastasis. Breast Cancer Res Treat. 2013; 138:741–52. [PubMed: 23539298]
31. Yu H, Simons DL, Segall I, Carcamo-Cavazos V, Schwartz EJ, Yan N, et al. PRC2/EED-EZH2 complex is up-regulated in breast cancer lymph node metastasis compared to primary tumor and correlates with tumor proliferation in situ. PLoS ONE. 2012; 7doi: 10.1371/journal.pone.0051239
32. Granit RZ, Gabai Y, Hadar T, Karamansha Y, Liberman L, Waldhorn I, et al. EZH2 promotes a bi-lineage identity in basal-like breast cancer cells. Oncogene. 2013; 32:3886–95. [PubMed: 22986524]
33. Dong C, Wu Y, Yao J, Wang Y, Yu Y, Rychahou PG, et al. G9a interacts with Snail and is critical for Snail-mediated E-cadherin repression in human breast cancer. J Clin Invest. 2012; 122:1469–86. [PubMed: 22406531]
34. Purcell DJ, Khalid O, Ou CY, Little GH, Frenkel B, Baniwal SK, et al. Recruitment of coregulator G9a by Runx2 for selective enhancement or suppression of transcription. J Cell Biochem. 2012; 113:2406–14. [PubMed: 22389001]
35. Wozniak RJ, Klimecki WT, Lau SS, Feinstein Y, Futscher BW. 5-Aza-2'-deoxycytidine-mediated reductions in G9A histone methyltransferase and histone H3 K9 di-methylation levels are linked to tumor suppressor gene reactivation. Oncogene. 2007; 26:77–90. [PubMed: 16799634]
36. Roll JD, Rivenbark AG, Jones WD, Coleman WB. DNMT3b overexpression contributes to a hypermethylator phenotype in human breast cancer cell lines. Mol Cancer. 2008; 7doi: 10.1186/14764598715
37. Buckley NE, Hosey AM, Gorski JJ, Purcell JW, Mulligan JM, Harkin DP, et al. BRCA1 regulates IFN- signaling through a mechanism involving the type I IFNs. Mol Cancer Res. 2007; 5:261–70. [PubMed: 17374731]
38. Hosey AM, Gorski JJ, Murray MM, Quinn JE, Chung WY, Stewart GE, et al. Molecular basis for estrogen receptor α deficiency in BRCA1 linked breast cancer. J Natl Cancer Inst. 2007; 99:1683–94. [PubMed: 18000219]

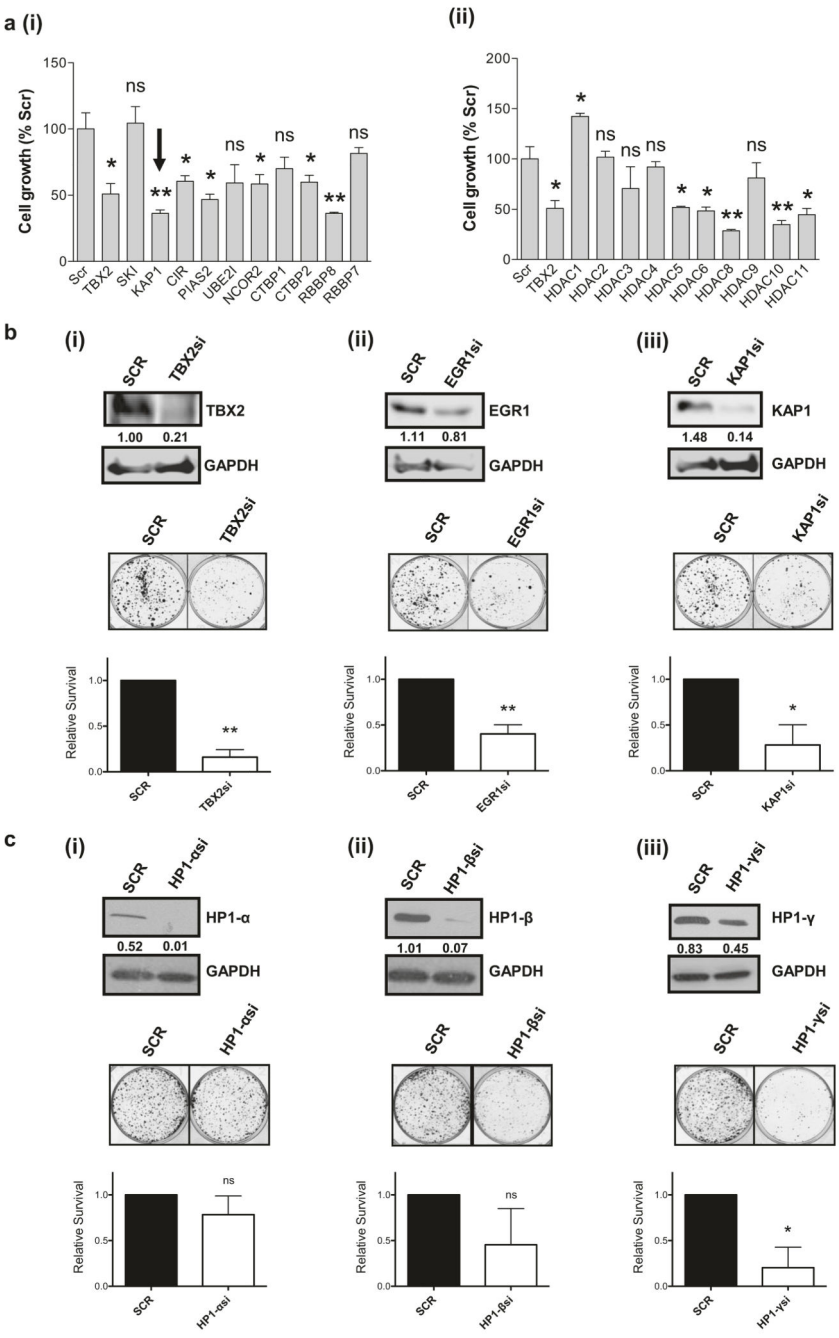

Fig. 1. Knockdown of KAP1/HP1 proteins inhibits the proliferation of MCF7 cells.

a Bar graphs representing growth of MCF7 cells screened with a panel of siRNAs against (i) co-repressor proteins, or (ii) Histone Deacetylases (HDACs). Cells were grown for 5 days prior to MTT assay. Each transfection was performed in triplicate and cell proliferation was calculated relative to scrambled control (Scr) siRNA (Cell growth %Scr) with TBX2 siRNA used as a positive control. Knockdown of KAP1 is highlighted with an inverted arrow. Error bars represent mean ± s.d. **b** MCF7 cells were treated for 7 days with siRNA against (i) TBX2, (ii) EGR1, or (iii) KAP1 alongside scrambled (SCR) control siRNA. Top panels

Europe PMC Funders Author Manuscripts

show western blot validation of knockdowns of respective target proteins, with GAPDH employed as a loading control. The effects of siRNA treatments on cell growth versus SCR control were assessed by crystal violet staining, the quantification of which is displayed below histograms. **c** MCF7 cells were treated for 7 days with siRNA against (i) HP1-α, (ii) HP1-β, or (iii) HP1-γ alongside scrambled (SCR) control siRNA. Top panels show western blot validation of knockdowns of respective target proteins, with GAPDH employed as a loading control. The effects of siRNA treatments on cell growth versus SCR control were assessed as before by crystal violet staining. Error bars represent mean ± s.d. of three independent experiments. $*P < 0.05$; $**P < 0.01$; ns = not significant compared with control

Europe PMC Funders Author Manuscripts

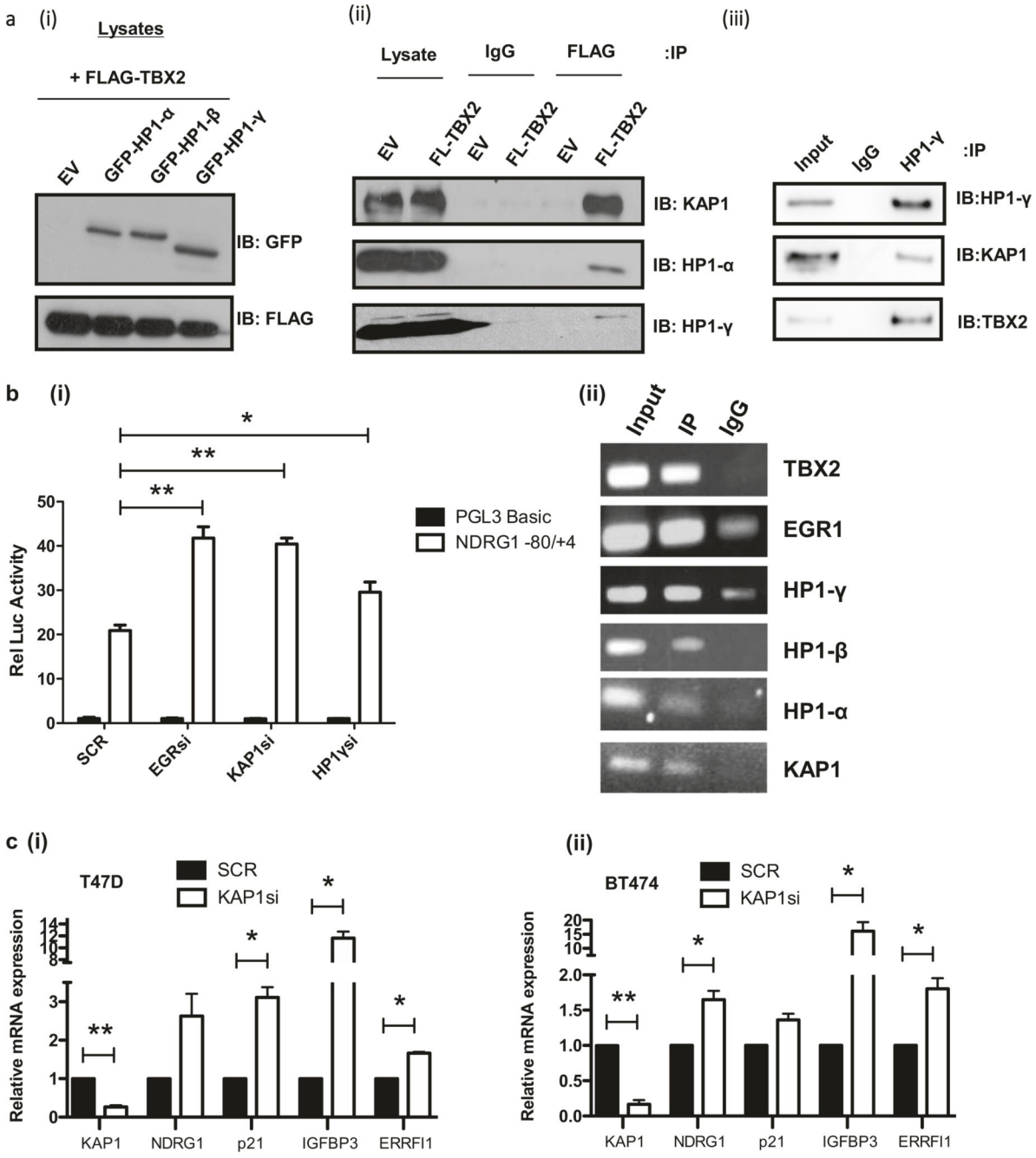

Fig. 2. TBX2 interacts with KAP1 and HP1 proteins to repress tumour suppressor genes.

a (i) Western blots showing MCF7 cell lysates following exogenous expression of GFP-tagged HP1 constructs alongside FLAG-tagged TBX2 and pulldowns performed with an anti-GFP antibody. Top panel shows westerns immunoblotted (IB) with GFP and bottom panel with an anti-FLAG antibody. (ii) Western blots of MCF7 cell lysates following exogenous expression of FLAG-tagged TBX2 followed by immunoprecipitation with an anti-FLAG antibody and IB for endogenous KAP1, HP1-α or HP1-γ. (iii) Endogenous co-IP using BT474 cell lysates immunoprecipitated with HP1-γ or isotype matched IgG

Europe PMC Funders Author Manuscripts

antibodies, the resultant western blots probed with HP1-γ antibody to demonstrate pulldown efficacy and antibodies specific for endogenous KAP1 (positive control) and TBX2. Input represents 30 μg of total protein. **b** (i) Bar graph showing luciferase reporter activities of an NDRG1 promoter construct (−80/+4) in MCF7 cells following transfection with siRNAs targeting EGR1, KAP1, or HP1-γ. Each transfection was performed in triplicate and a Renilla luciferase construct was used as transfection control, with an empty vector (pGL3 basic) also shown for each treatment. Error bars represent mean ± s.e.m. (ii) ChIP assays of endogenous TBX2, EGR1, KAP1 and HP1 proteins for the NDRG1 promoter in MCF7 cells. Input represents 5% of lysate prior to ChIP and an isotype-matched IgG served as a negative control ChIP. **c** Bar graphs of RqPCR values demonstrating siRNA knockdown of KAP1 in T47D cells at 120 h (i) and in BT474 cells at 96 h (ii) versus scrambled (SCR) control with resulting effects on expression of TBX2 and EGR1-target genes. SDHA mRNA was used to normalise values. Error bars represent mean ± s.e.m. of three independent experiments. $*P < 0.05$; $**P < 0.01$

Europe PMC Funders Author Manuscripts

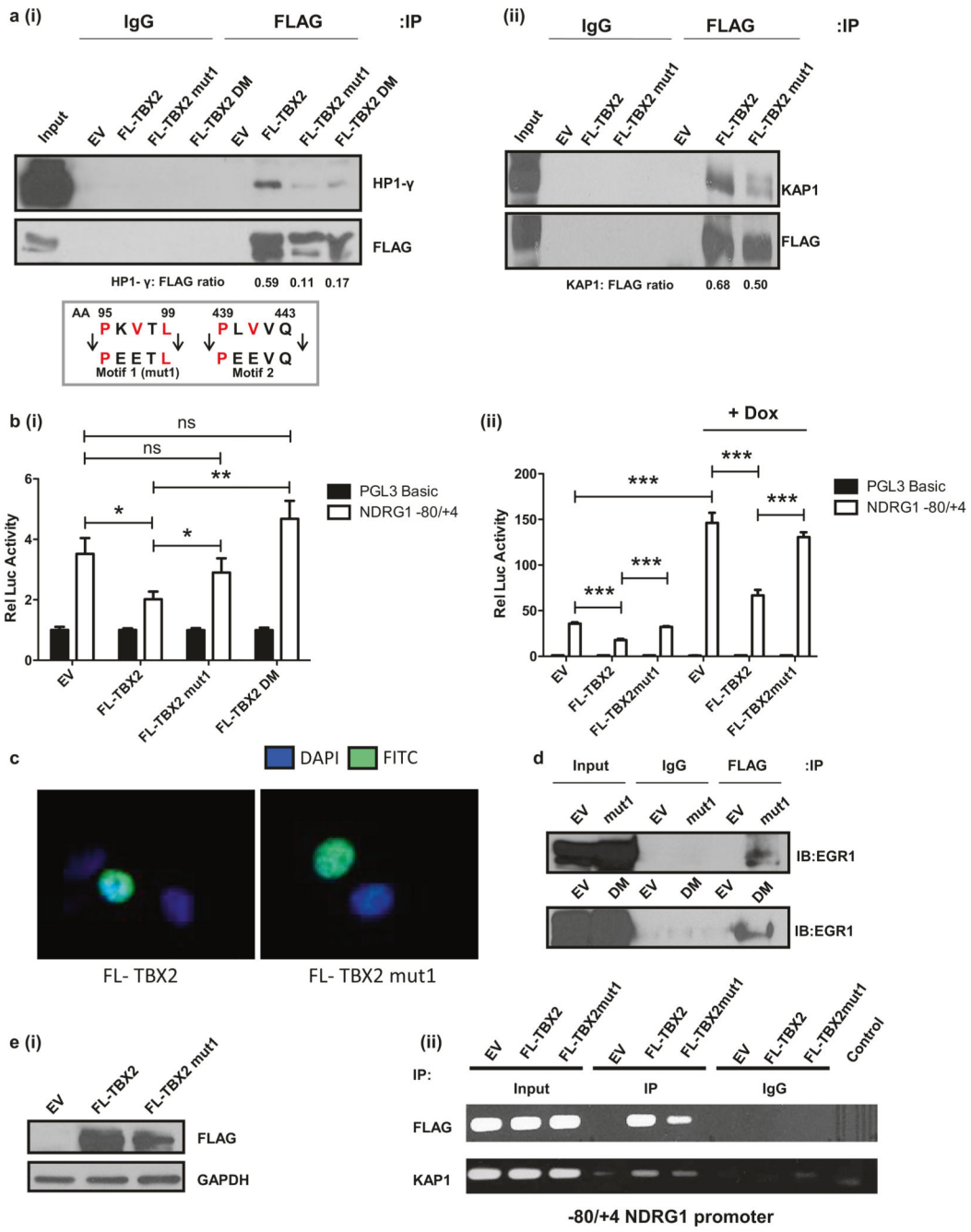

Fig. 3. TBX2 specifically interacts with HP1 to recruit KAP1 and repress the NDRG1 promoter.

a (i) Western blot of MCF7 cell lysates following exogenous expression of empty vector (EV), FLAG-tagged wild-type TBX2 (FL-TBX2), a FLAG-tagged single HP1 site point mutant TBX2 (FL-TBX2 mut1), or a FLAG-tagged double HP1 site point mutant TBX2 (FL-TBX2 DM). Locations of the two HP1 binding motifs on TBX2 where SDM was performed are detailed in below schematic (key residues highlighted in red), with TBX2 DM containing both of the described mutations. Pulldowns were performed with an anti-FLAG antibody and the resultant blot was immunoblotted for endogenous HP1-γ. (ii) Western blot

of MCF7 cell lysates following exogenous expression of empty vector (EV), FLAG-tagged wild-type TBX2 (FL-TBX2), or a FLAG-tagged single HP1 site point mutant TBX2 (FL-TBX2 mut1). Pulldowns were performed with an anti-FLAG antibody and the resultant blot was immunoblotted for endogenous KAP1. Below densitometric values demonstrate amount of co-immunoprecipitated protein normalised to FLAG-tagged TBX2. **b** (i) Bar graph showing luciferase reporter activities of an NDRG1 promoter construct (−80/+4) in MCF7 cells following transfection with the constructs outlined in **a**. Each transfection was performed in triplicate and a Renilla luciferase construct was used as transfection control with an empty vector (pGL3 basic) also shown for each treatment. (ii) Bar graph showing luciferase reporter activities of an NDRG1 promoter construct (−80/+4) in MCF7 cells following transfection of an empty vector (EV), a FLAG-tagged wild-type TBX2 (TBX2), or a FLAG-tagged single HP1 site point mutant TBX2 (TBX2/HP1 mutant). Cells were left untreated or treated with 1 μM doxorubicin (+Dox) for 24 h prior to measurement of luciferase activities. Each transfection was performed in triplicate and a Renilla luciferase construct was used as transfection control with an empty vector (pGL3 basic) also shown for each treatment. Error bars represent mean ± s.e.m. *P<0.05; **P<0.01; ***P 0.001; ns = not significant. **c** Immunofluorescence microscopy images showing MCF7 cells transfected with a FLAG-tagged wild-type TBX2 (FL-TBX2) or a FLAG-tagged single HP1 site point mutant TBX2 (FL-TBX2 mut1). A FITC-conjugated secondary antibody (green) shows transfected cells with both constructs localising to the nucleus whilst DAPI counterstaining was used to show nuclei. **d** Western blot showing MCF7 cell lysates following exogenous expression of empty vector (EV), single (top panel, mut1) or double (bottom panel, DM) HP1 site point mutant, FLAG-tagged TBX2. Pulldowns were performed with an anti-FLAG antibody (alongside isotype matched IgG as negative control) and the resultant blots were probed with an anti-EGR1 antibody. **e** (i) Western blot of MCF7 cell lysates showing exogenous expression of empty vector (EV), FLAG-tagged wild-type TBX2 (FLTBX2), or a FLAG-tagged single HP1 site point mutant TBX2 (FLTBX2 mut1). GAPDH serves as a loading control. (ii) ChIP assays of the −80/+4 NDRG1 proximal promoter (cells transfected as described in (i)) using anti-FLAG and anti-KAP1 antibodies alongside isotype matched IgG antibodies. Input represents 5% of lysate prior to pulldowns with water as a negative control (control lane)

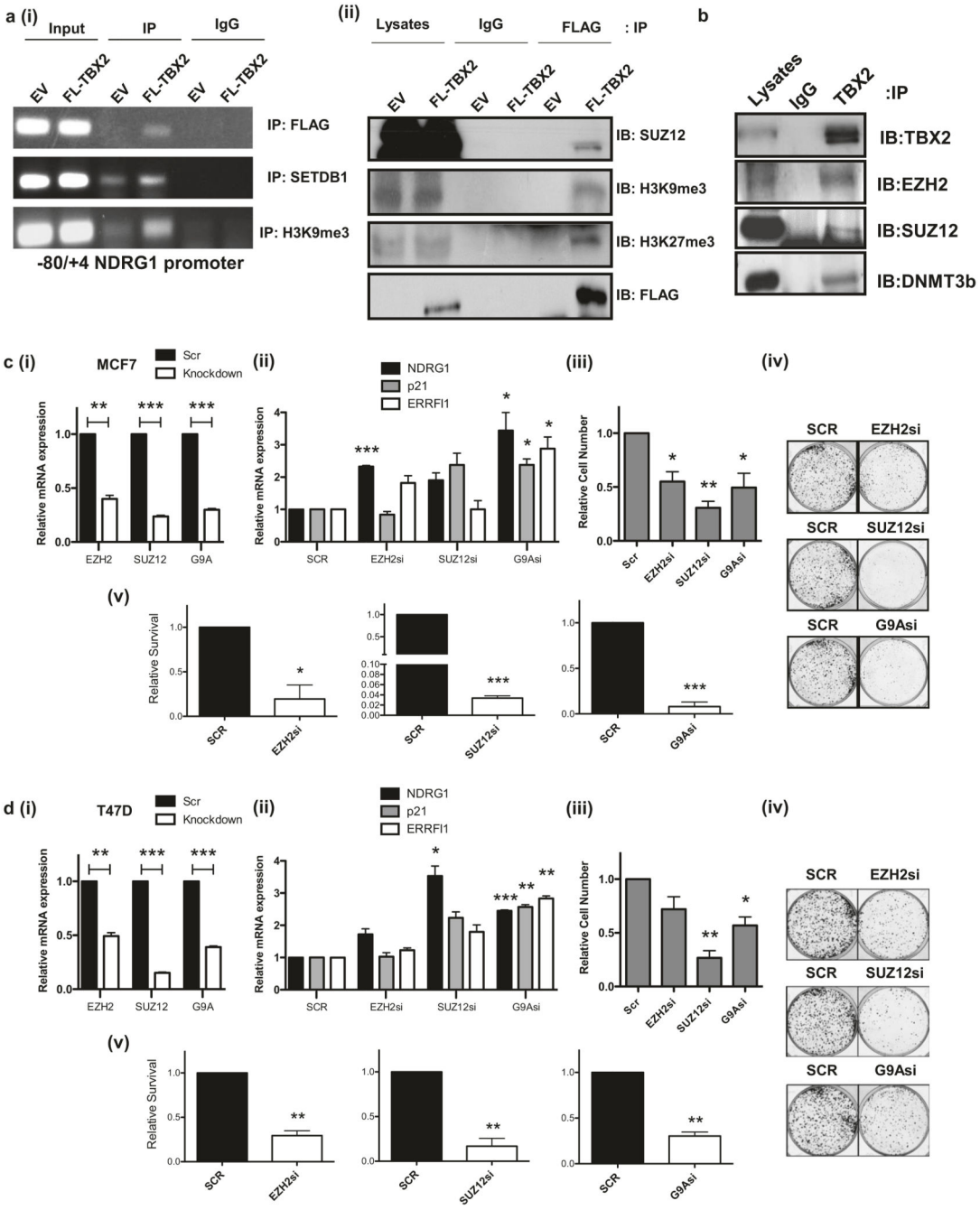

Fig. 4. TBX2 recruits repressors and negative chromatin marks to target promoters.

a (i) ChIP assays of MCF7 cells following transfection of empty vector (EV) and FLAG-tagged wild-type TBX2 (FLTBX2) constructs with ChIP primers spanning the −80/+4 NDRG1 proximal promoter. Pulldowns were performed using anti-FLAG, anti-SETDB1 and anti-H3K9me3 antibodies with an isotype matched IgG antibody as negative control. Input represents 5% of lysate prior to pulldowns. (ii) U2OS cells were transfected and pulldowns performed as described in (i), which were immunoblotted using antibodies specific for the PRC2 component SUZ12 and the chromatin marks H3K9me3 and K27me3, with FLAG

Europe PMC Funders Author Manuscripts

showing exogenous FL-TBX2 expression. **b** Western blots showing endogenous co-IP experiments using MCF7 cell lysates immunoprecipitated with TBX2 or isotype matched IgG antibodies, the resultant blots probed with TBX2 antibody to demonstrate pulldown efficacy and antibodies specific for several members of the proposed repression complex (SUZ12, EZH2 and DNMT3B). Lysates (30 μg of total protein) shows the endogenous expression of each protein. **c** (i) Bar graph of RqPCR values demonstrating the efficacies of siRNA knockdowns of EZH2, SUZ12 and G9A at 96 h in MCF7 cells versus scrambled (Scr) control. SDHA mRNA was used to normalise values. (ii) Bar graph of mRNA of TBX2/EGR1-target genes matched to samples outlined in (i), normalised to SDHA mRNA. Error bars represent mean ± s.e.m. of three independent experiments. (iii) Cell counts matched to RqPCR experiments at 96 h transfection with previously outlined siRNAs. Error bars represent mean ± s.d. of three independent experiments. (iv) Representative scans of crystal violet-stained MCF7 cells 11 days post-treatment with previously described siRNAs alongside scrambled control (SCR) siRNA. (v) Relative survival assessed by quantification of crystal violet staining following EZH2/SUZ12/G9A knockdown. Error bars represent mean ± s.d. of three independent experiments. **d** (i) Bar graph of RqPCR values demonstrating the efficacies of siRNA knockdowns of EZH2, SUZ12 and G9A at 120 h in T47D cells versus scrambled (Scr) control. SDHA mRNA was used to normalise values. (ii) Bar graph of mRNA of TBX2/EGR-target genes matched to samples outlined in (i), normalised to SDHA mRNA. Error bars represent mean ± s.e.m. of three independent experiments. (iii) Cell counts matched to RqPCR experiments at 120 h transfection with previously outlined siRNAs. Error bars represent mean ± s.d. of three independent experiments. (iv) Representative scans of crystal violetstained T47D cells 19 days post-treatment with previously described siRNAs alongside scrambled control (SCR) siRNA. (v) Relative survival assessed by quantification of crystal violet staining following EZH2/SUZ12/G9A knockdown. Error bars represent mean ± s.d. of three independent experiments. $*P<0.05$; $**P<0.01$; $***P<0.001$ compared with control for all charts

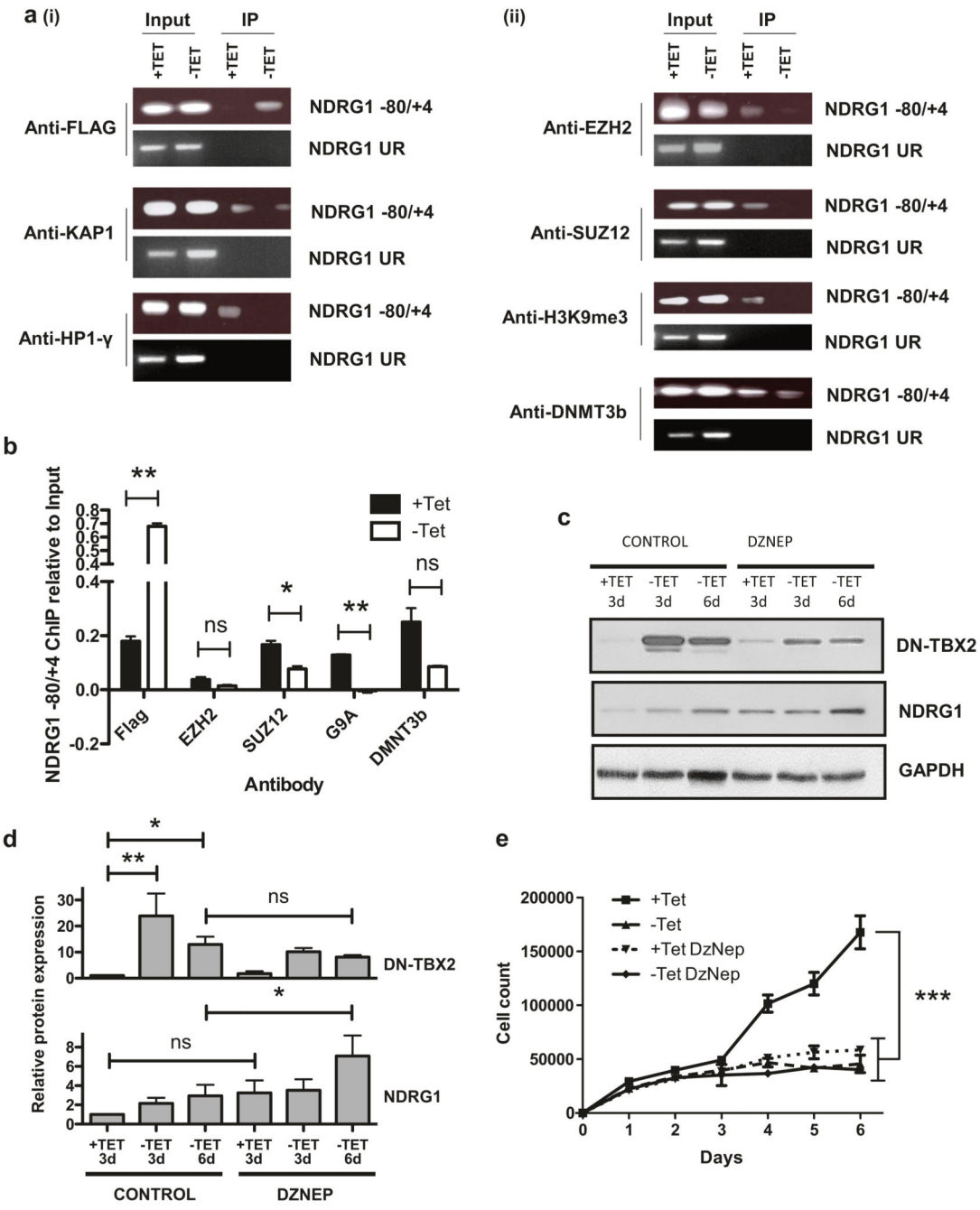

Fig. 5. Inhibition of TBX2 abrogates HMT and DNMT recruitment to target promoters and impairs proliferation of breast cancer cells.

a ChIP assays of MCF7-DN cells following tetracycline induction of a dominant-negative TBX2 (-TET) compared to uninduced (+TET) cells using ChIP primers spanning the −80/+4 NDRG1 proximal promoter. Pulldowns were performed using (i) anti-FLAG, anti-KAP1, anti-HP1γ and (ii) anti-EZH2, anti-SUZ12, anti-H3K9me3 and DNMT3B antibodies. A negative control using primers designed against a non-specific genomic region approximately 1 kb upstream of the NDRG1 promoter (NDRG1 UR) was also used. Input

represents 5% of lysate prior to pulldowns. **b** Bar graph of RqPCR measurements of ChIP DNA taken from ChIP assay described in **a**, assessing enrichment of DN-TBX2 on the NDRG1 promoter (FLAG) and the effects on recruitment of EZH2, SUZ12, G9A and DNMT3B (−TET versus +TET). The experiment was performed in duplicate and error bars represent mean ± s.e.m. **c** Western blots of 3 day and 6 day induction of DN-TBX2 assessing effects on expression of NDRG1, in the presence or absence of generic HMT inhibitor DzNep. **d** Densitometric quantification of DN-TBX2 and NDRG1 protein expression from western experiments outlined previously in **c**, normalised to 3 day + TET control. Error bars represent mean ± s.d. of two independent experiments. **e** Graph showing MCF-DN growth curves over a six day period without (+Tet) or with (−Tet) induction of DN-TBX2, and with/without co-treatment with 1 μM DzNep. The experiment was performed in triplicate and error bars represent mean ± s.d. *P<0.05 **P<0.01; ***P<0.001; ns = not significant

Europe PMC Funders Author Manuscripts

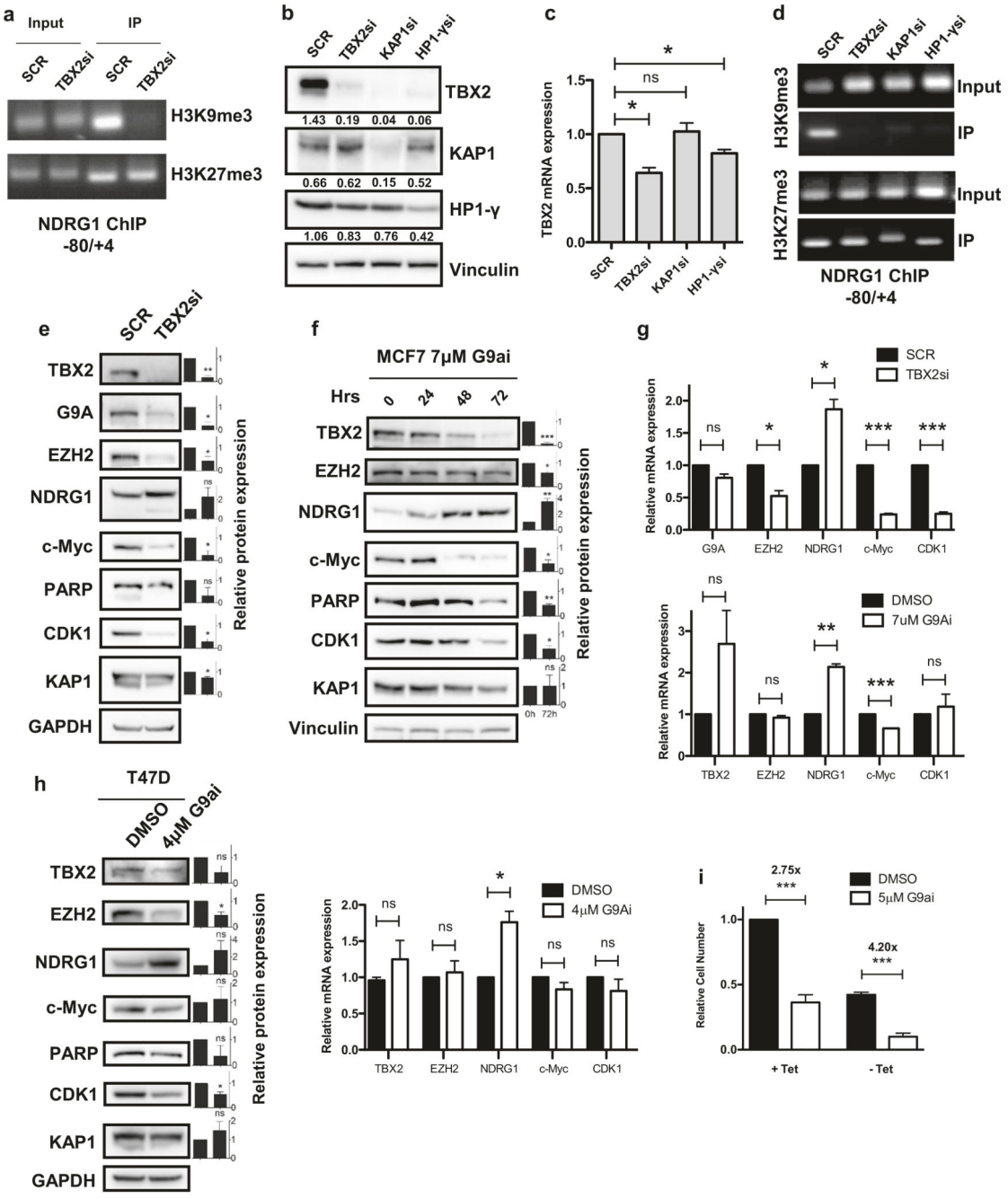

Fig. 6. The TBX2/KAP1/HP1-γ complex specifically mediates H3K9 trimethylation of the NDRG1 promoter to sustain growth and survival of breast cancer cells.

a ChIP assay of MCF7 cells following 72 h treatment with TBX2 siRNA using ChIP primers spanning the −80/+4 NDRG1 proximal promoter. Pulldowns were performed using anti-H3K9me3 antibody in comparison with anti-H3K27me3 antibody. **b** MCF7 cells were treated for 72 h with siRNAs against TBX2, KAP1 and HP1-γ. Knockdown efficacy was assessed at the protein level by western blot analysis, with Vinculin as a loading control. **c** TBX2 mRNA levels in samples matched to **b** were measured by RqPCR. SDHA mRNA was

Europe PMC Funders Author Manuscripts

used to normalise values. Error bars represent mean ± s.e.m. of three independent experiments. **d** ChIP assay matched to knockdown experiment as described in **b** using primers spanning the NDRG1 proximal promoter. The effect of TBX2/KAP1/HP1-γ knockdown on NDRG1 promoter methylation was assessed by pulldown with anti-H3K9me3 antibody, while anti-H3K27me3 antibody was employed as a negative control. **e** MCF7 cells were treated with TBX2 siRNA as described in **a**. Western blot was performed on lysates to assess the downstream effects on protein levels of histone methyltransferases (G9A, EZH2), tumour suppressors (NDRG1) and anti-senescence proteins (c-Myc, PARP, CDK1, KAP1). GAPDH antibody serves as a loading control. Adjacent bar graphs represent mean ± s.d. of densitometric readings from three independent experiments normalised to loading control. **f** MCF7 cells were treated for 72 h with G9A inhibitor BIX-01294. Western blot was performed on lysates to assess downstream effects on levels of TBX2, tumour suppressors and anti-senescence proteins as described previously. Adjacent bar graphs comparing 0 h to 72 h represent mean ± s.d. of densitometric readings from three independent experiments normalised to loading control. **g** RqPCR measurement of mRNA levels from samples matched to MCF7 experiments in **e** and **f**, respectively. SDHA mRNA was used to normalise values. Error bars represent mean ± s.e.m. of three independent experiments. **h** T47D cells were treated for 72 h with DMSO or G9A inhibitor BIX-01294. Western blot was performed to assess downstream effects on levels of TBX2, tumour suppressors and anti-senescence proteins as described previously. Adjacent bar graphs represent mean ± s.d. of densitometric readings from three independent experiments normalised to loading control. RqPCR was performed on matched mRNA with SDHA mRNA levels used to normalise values. Error bars represent mean ± s.e.m. of three independent experiments. **i** MCF7-DN cells were induced to express DN-TBX2 (−Tet) or left uninduced (+Tet) for 2 days prior to treatment with DMSO or G9A inhibitor BIX-01294 for a further 3 days. Graphs demonstrate effects on cell number relative to the uninduced DMSO control. Fold change in cell number with G9A inhibition relative to DMSO-treated cells is shown for the +Tet and −Tet groups. Error bars represent mean ± s.d. of three independent experiments. *P<0.05; **P<0.01; ***P<0.001; ns = not significant for all charts

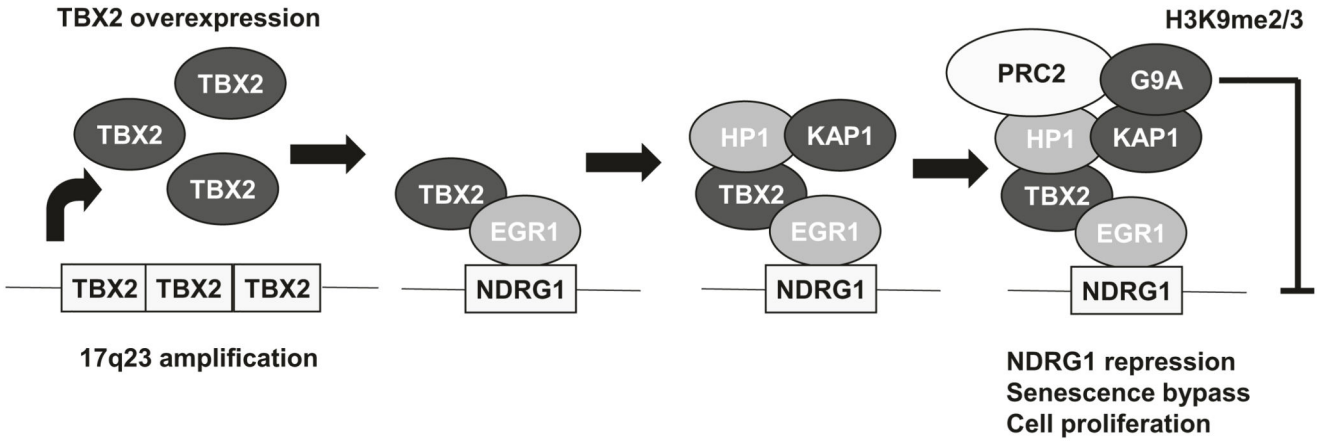

Fig. 7. Schematic of proposed TBX2-dependent repression of NDRG1

Europe PMC Funders Author Manuscripts